nature metabolism

Supplementary information

https://doi.org/10.1038/s42255-026-01599-5

Multi-organ proteomic atlas of obesity regression in male mice

In the format provided by the authors and unedited

Table of Contents

Supplementary Figures

Supplementary Fig. S1 | Overview of sample depth. Number of unique proteins identified per sample across tissues.

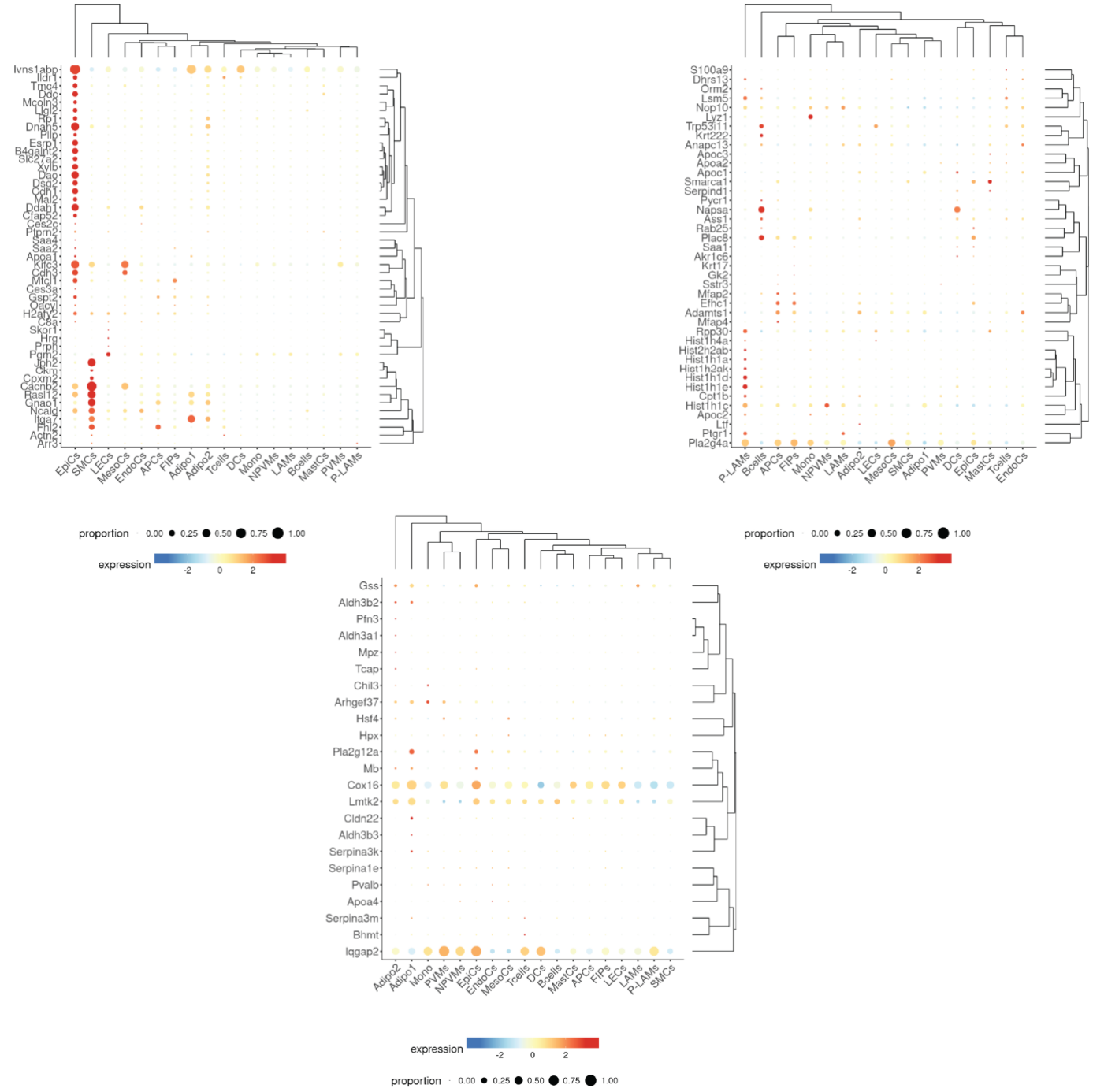

Supplementary Fig. S2 | Cell-type contextualization of RNA-protein discordant proteins in eWAT. Proteins showing opposite-direction regulation at the protein and transcript levels were mapped to a matched single-nucleus RNA-seq dataset from epididymal adipose tissue under a comparable obesity and weight loss paradigm (Hinte et al., Nature 2024). Selected proteins had shown upregulation in protein-level but downregulation on the RNA-level, corresponding to proteins colored red Extended Data Fig. 4a. Normalized and scaled gene expression (color scale) and fraction of nuclei (dot size) across annotated cell types. Plots were generated using the Hinte et al. (Nature 2024) web application, split in three as a result of limitations in the web application.

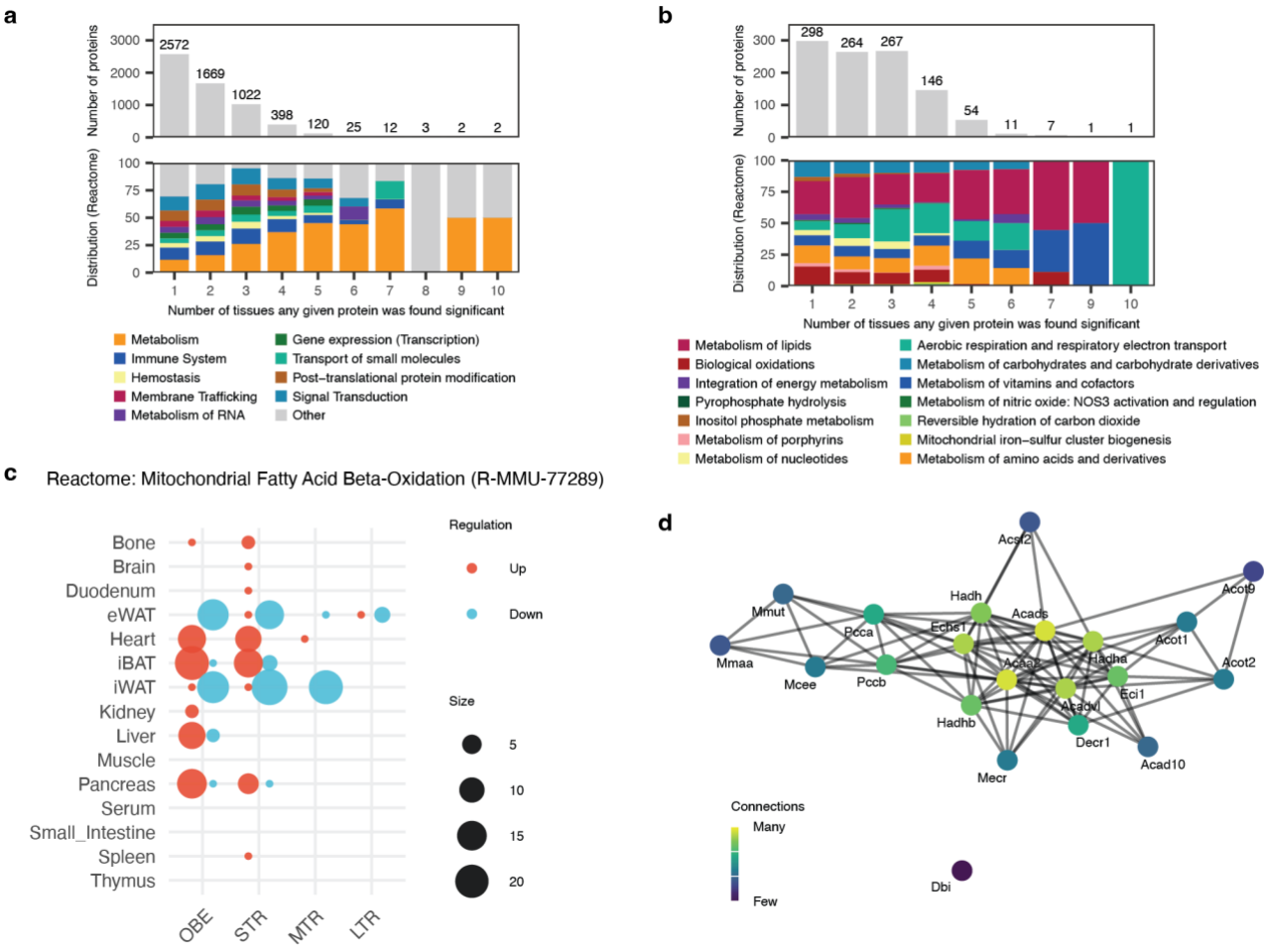

Supplementary Fig. S3 | Pathway analysis of DEPs based on number of tissues they were shared in. a, Bar plot (top) shows the count of DEPs shared in N number of tissues, distribution plot (bottom) shows which Reactome parent pathway the DEPs found in N number of tissues belonged to. **b,** Similar to **a** but one layer deeper, so bar plot (top) shows the count of DEPs related to metabolism found in N number of tissues, and distribution plot (bottom) shows the Reactome first-child pathways of 'Metabolism' the DEPs in each group belonged to. **c,** Dot plot showing system-wide distribution for DEPs belonging to the Reactome pathway 'Mitochondrial Fatty Acid Beta-Oxidation' (R-MMU-77289). **d,** STRING Network plot of the 'Mitochondrial Fatty Acid Beta-Oxidation' DEPs shared in 4 or more tissues. OBE obese, STR short-term regression, MTR medium-term regression, LTR long-term regression. Figure panel **c** was generated using our web application (https://computproteomics.bmb.sdu.dk/app_direct/obesity-atlas/).

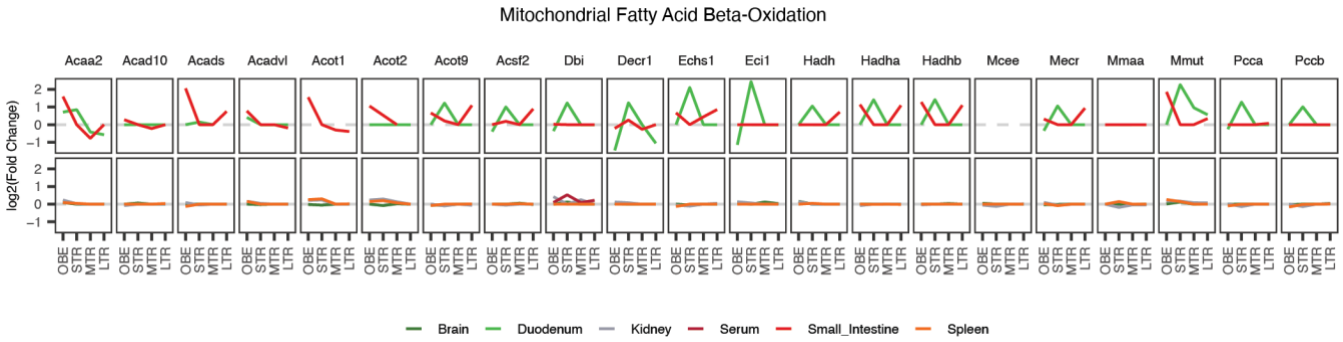

Supplementary Fig. S4 | Remaining expression profiles for 'Mitochondrial Fatty Acid Beta-Oxidation'. Expression profiles showing estimated $\log_2$ fold changes (biological replicates: obesity, n = 5; corresponding lean controls, n = 6; all regression and corresponding control groups, n = 6) for 'Mitochondrial Fatty Acid Beta-Oxidation' DEPs shared across 4 or more tissues. Displayed tissues are brain, duodenum, kidney, serum, small intestine, and spleen. Remaining tissues can be found in main Fig. 3. OBE obese, STR short-term regression, MTR medium-term regression, LTR long-term regression.

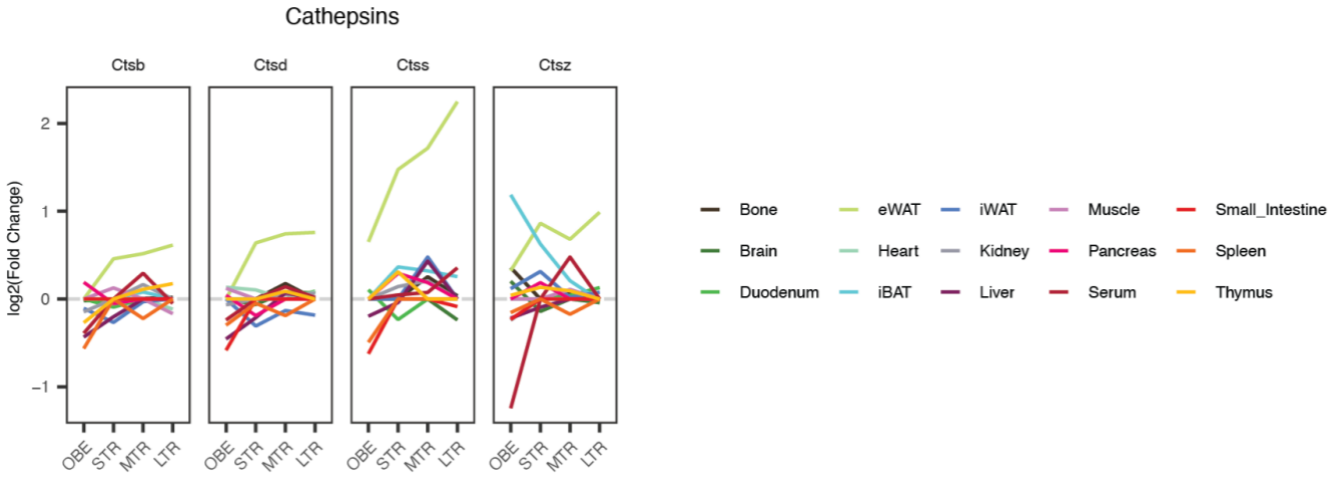

Supplementary Fig. S5 | Analysis of autolysis. Expression profiles showing estimated $\log_2$ fold changes (biological replicates: obesity, n = 5; corresponding lean controls, n = 6; all regression and corresponding control groups, n = 6) for cathepsins across each tissue. OBE obese, STR short-term regression, MTR medium-term regression, LTR long-term regression. Figure was generated using our web application (https://computproteomics.bmb.sdu.dk/app_direct/obesity-atlas/).

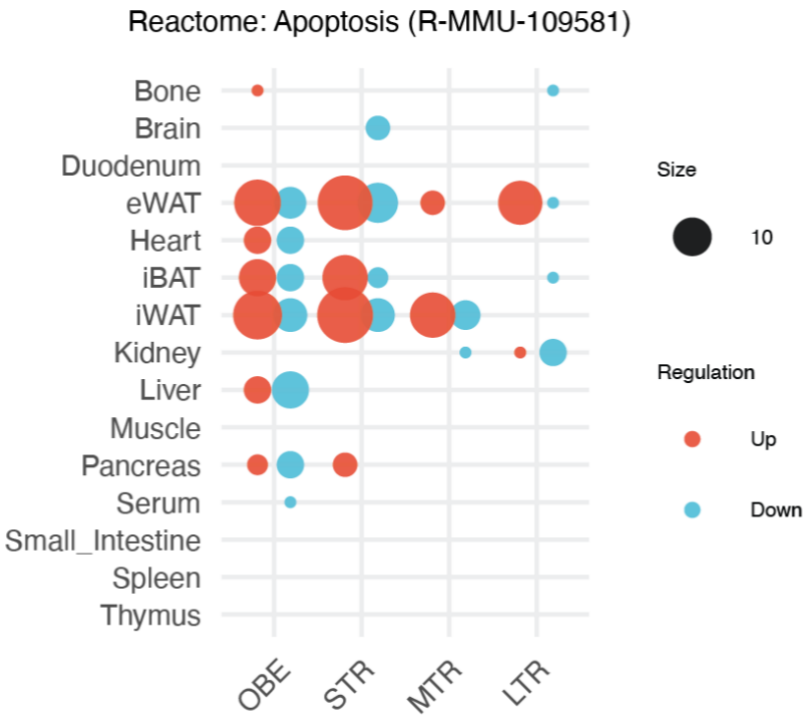

Supplementary Fig. S6 | Analysis of apoptosis. Dot plot showing the system-wide DEP count for proteins in the Reactome pathway 'Apoptosis' (R-MMU-109581). OBE obese, STR short-term regression, MTR medium-term regression, LTR long-term regression. Figure was generated using our web application (https://computproteomics.bmb.sdu.dk/app_direct/obesity-atlas/).

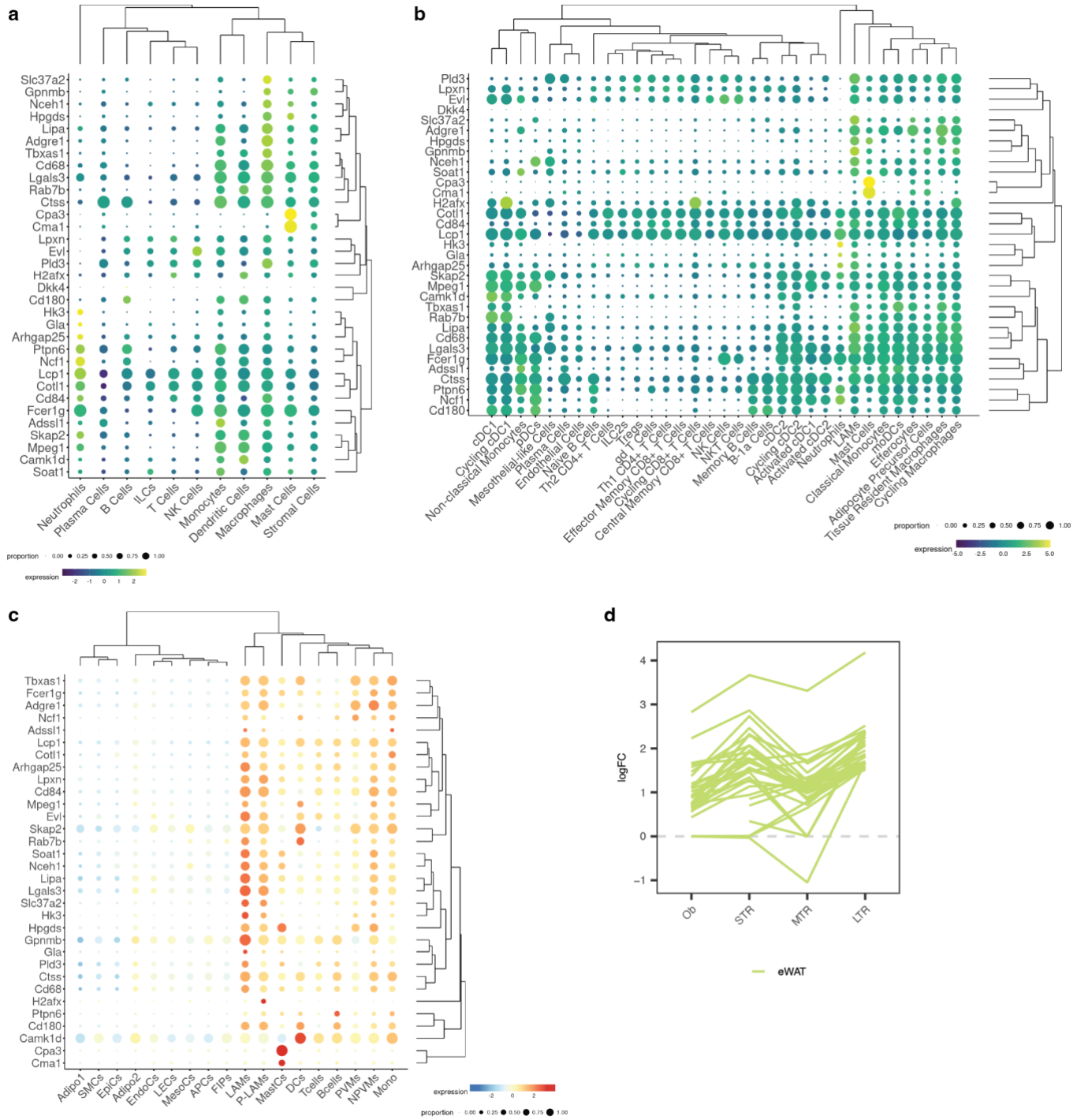

Supplementary Fig. S7 | Cell-type context of proteins persistently upregulated in eWAT during long-term regression of obesity. a-b, Expression of genes corresponding to proteins most upregulated in eWAT during long-term regression mapped onto a published single-cell adipose immune atlas (Cottam et al., Nature Communications 2022). **a,** Shows major immune cell classes, whereas **b,** shows finer immune subpopulations. **c,** Expression of the same gene set across stromal and parenchymal adipose cell types from a snRNA-seq atlas of eWAT (Hinte et al., Nature 2024). **a-c,** Dot size indicates the fraction of cells and color scale represents normalized and scaled expression levels. **d,** Expression profile showing estimated $\log_2$ fold changes (biological replicates: obesity, n = 5; corresponding lean controls, n = 6; all regression and corresponding control groups, n = 6) for proteins upregulated in LTR of eWAT. Figure panels **a** and **b** were generated using the Cottam et al. (Nature Communications 2022) web application. Figure panel **c** was generated using the Hinte et al. (Nature 2024) web application. Figure panel **d** was generated using our web application (https://computproteomics.bmb.sdu.dk/app_direct/obesity-atlas/).

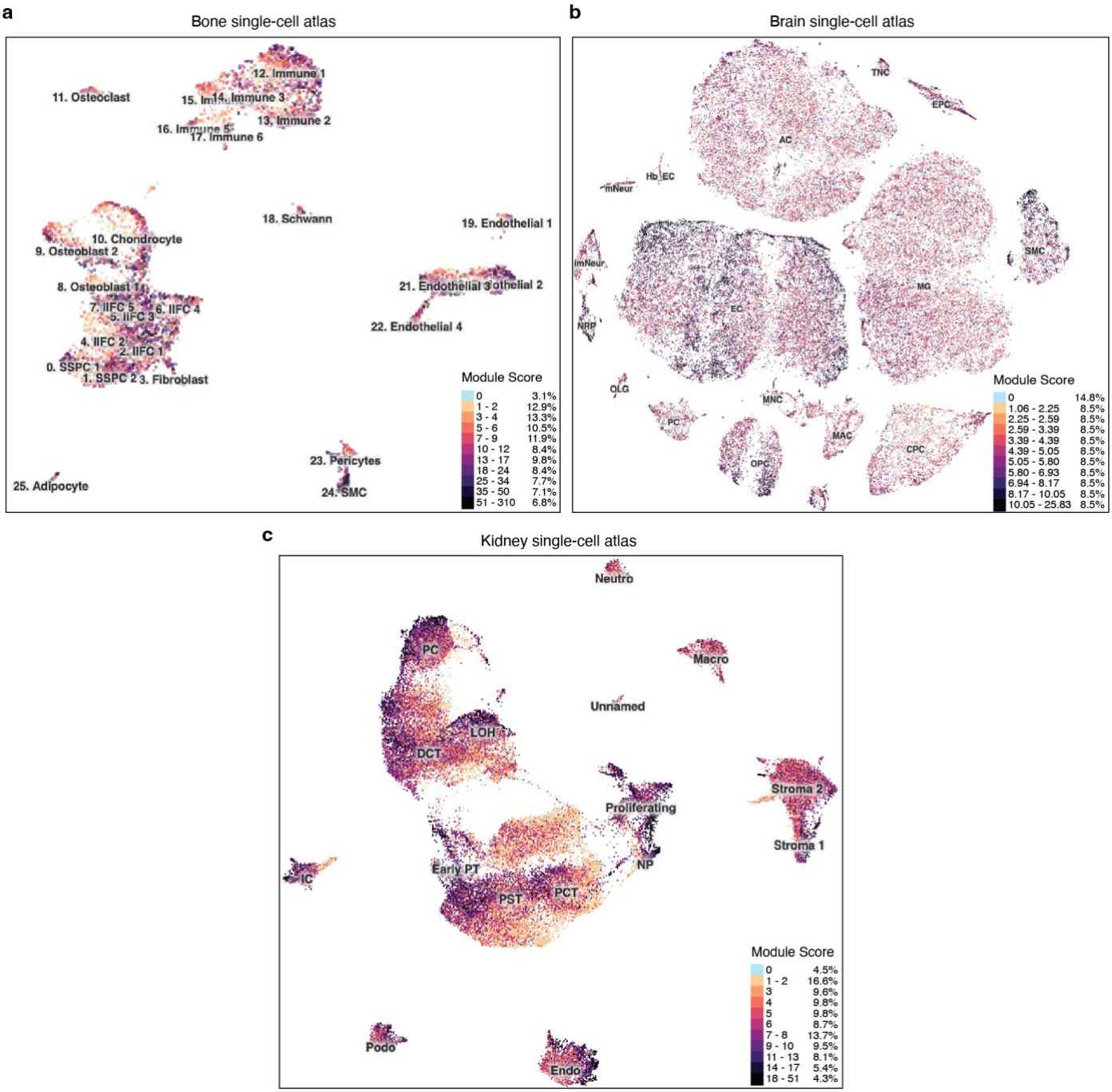

Supplementary Fig. S8 | Cellular distribution of the cross-tissue module. Public single-cell RNA-seq atlases of **a,** bone (Perrin et al., eLife 2024), **b,** brain (Zhao et al., BioRxiv 2019), and **c,** kidney (Miao et al., Nature Communications 2021) were queried for the protein module / STRING network (Fig. 3i) identified as being coordinately downregulated across these tissues during long-term regression of obesity. Plots were generated using the UCSC Cell Browser (Speir et al., Bioinformatics 2021). Cells are colored by their module score (summed normalized expression of Fig. 3i genes). Cell-type labels follow the original atlas annotations. These maps indicate cellular compartments expressing this protein module and are not differential expression analysis.

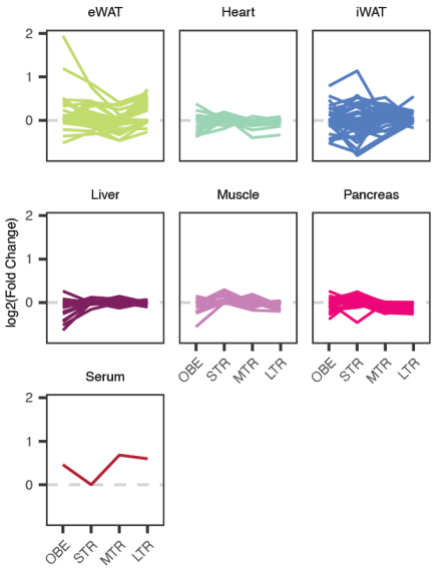

Supplementary Fig. S9 | Analysis of expression in remaining tissues. Expression profiles showing estimated log_2 fold changes (biological replicates: obesity, n = 5; corresponding lean controls, n = 6; all regression and corresponding control groups, n = 6) for the 42 DEPs highlighted in the intersections from (Fig. 4g) for the remaining tissues not already shown in (Fig. 4h). OBE obese, STR short-term regression, MTR medium-term regression, LTR long-term regression. Figure was generated using our web application (https://computproteomics.bmb.sdu.dk/app_direct/obesity-atlas/).

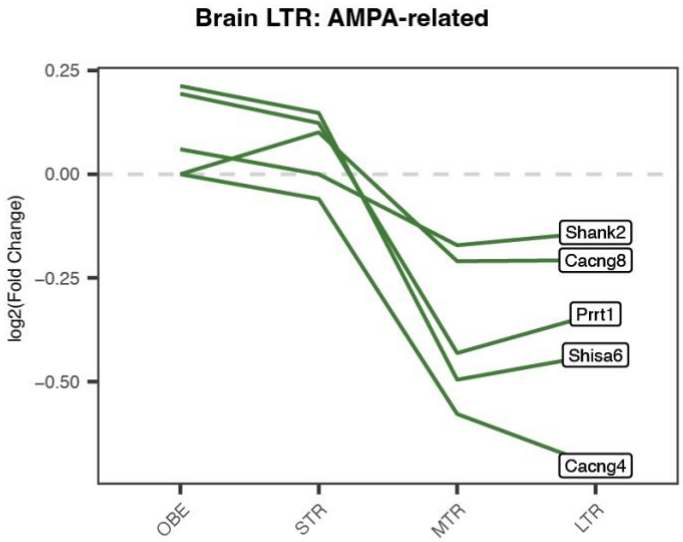

Supplementary Fig. S10 | AMPA-related proteins. Expression profiles showing estimated log_2 fold changes (biological replicates: obesity, n = 5; corresponding lean controls, n = 6; all regression and corresponding control groups, n = 6) for for various DEPs found significant in LTR of brain. OBE obese, STR short-term regression, MTR medium-term regression, LTR long-term regression.

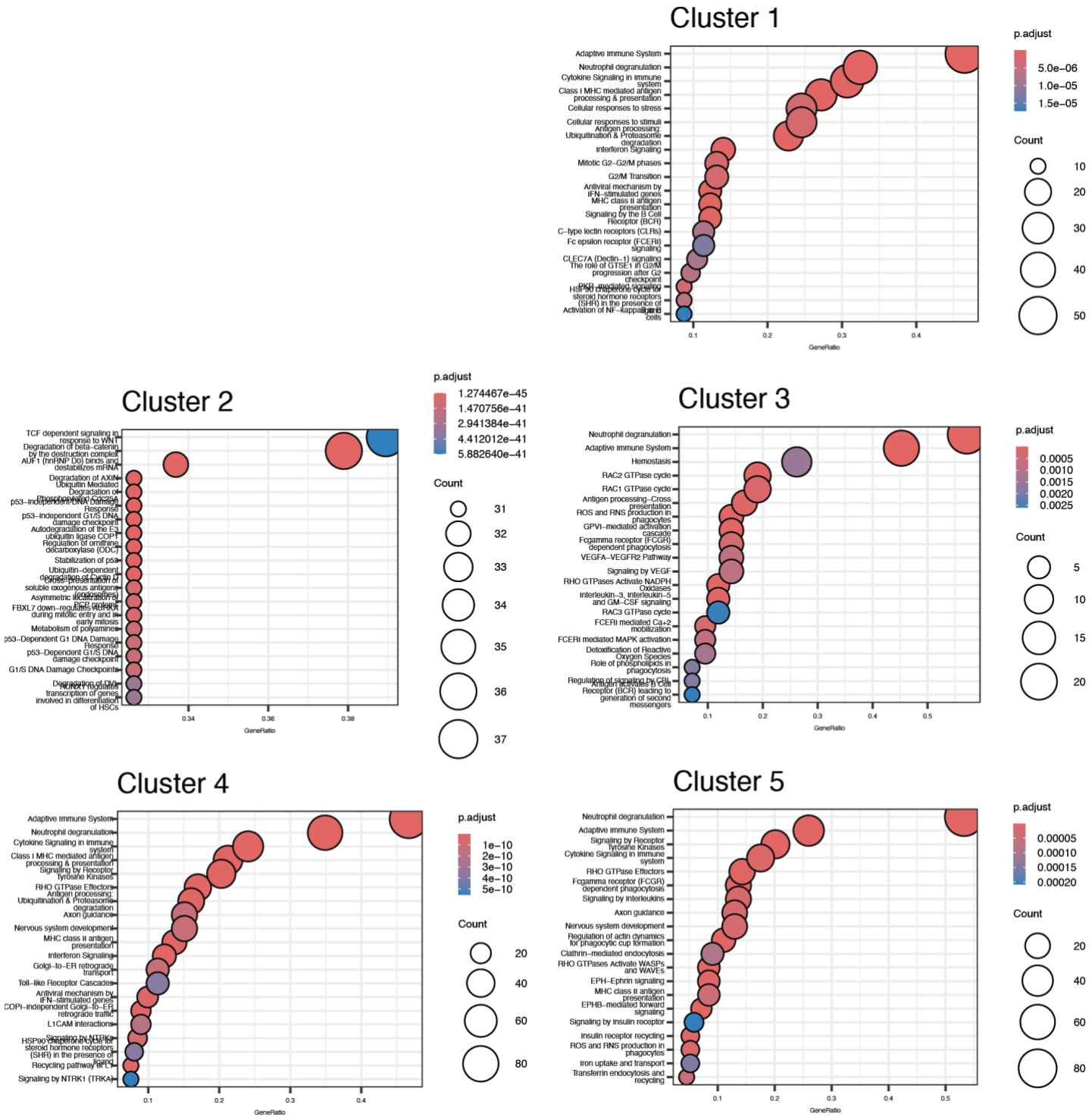

Supplementary Fig. S11 | Pathway analysis of adipose tissue immune system DEP clusters. Dot plots for the Reactome pathway enrichment analysis of the clusters in (Fig. 6a).

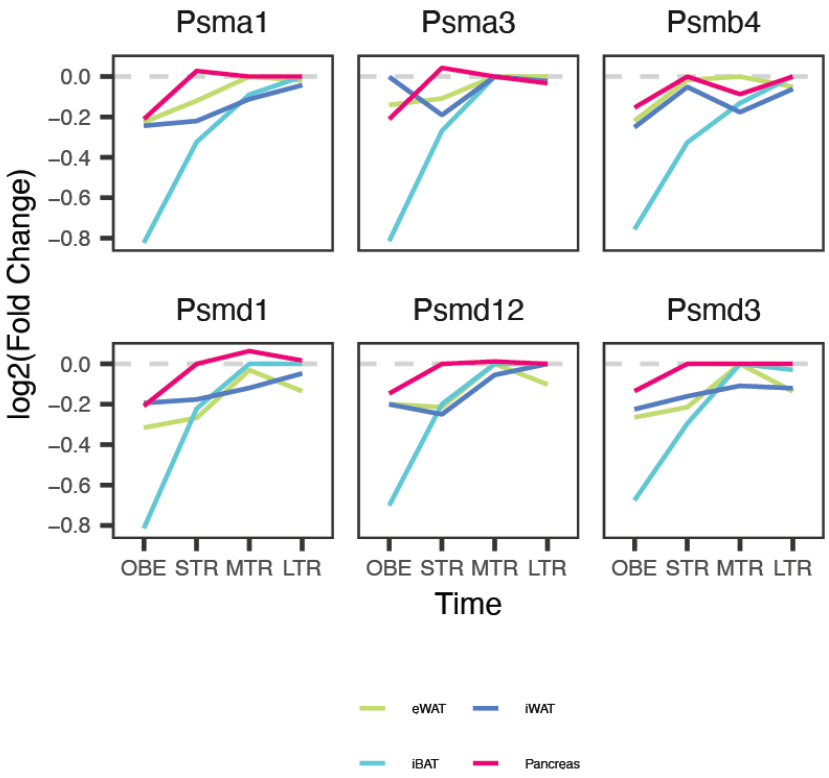

Supplementary Fig. S12 | Proteasome downregulation. Expression profiles showing estimated $\log_2$ fold changes (biological replicates: obesity, n = 5; corresponding lean controls, n = 6; all regression and corresponding control groups, n = 6) for various proteasomal subunits. OBE obese, STR short-term regression, MTR medium-term regression, LTR long-term regression. Figure was generated using our web application (https://computproteomics.bmb.sdu.dk/app_direct/obesity-atlas/).

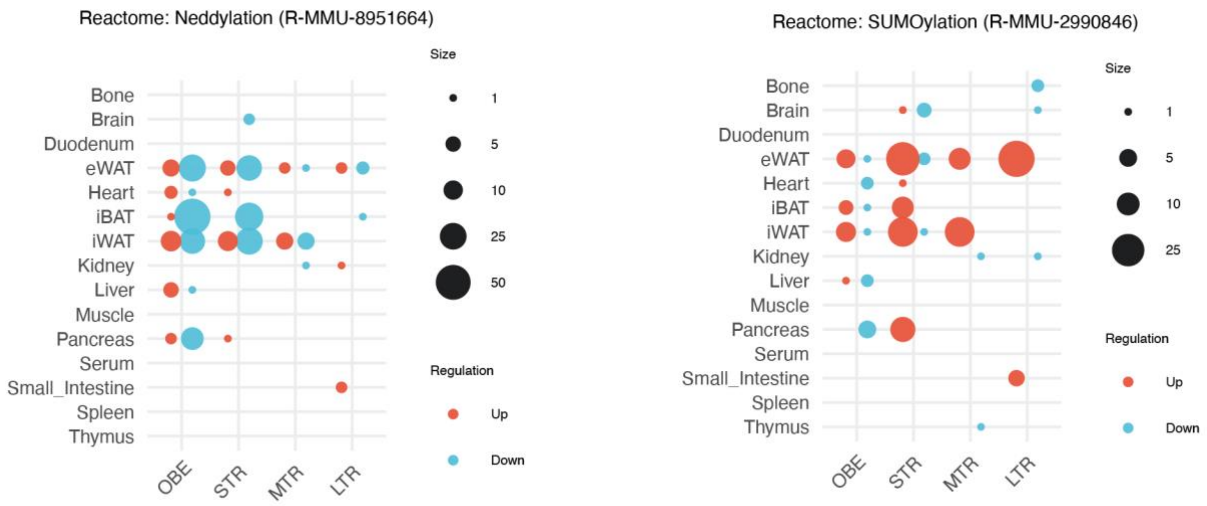

Supplementary Fig. S13 | Exploring system-wide post-translational modifications. Dot plots showing the system-wide DEP count for proteins in the Reactome pathways 'Neddylation' (left) and 'SUMOylation' (right). OBE obese, STR short-term regression, MTR medium-term regression, LTR long-term regression. Figure was generated using our web application (https://computproteomics.bmb.sdu.dk/app_direct/obesity-atlas/).

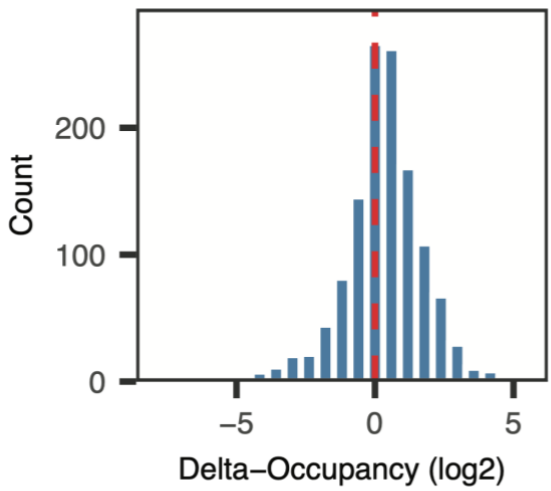

Supplementary Fig. S14 | Global ubiquitin delta occupancy. Histogram for the delta occupancy between obese and lean control mice, showing a positive shift towards obese. A one-sided Wilcoxon signed-rank test with continuity correction confirmed that Delta-occupancy values were significantly shifted above zero ($p < 2.2e-16$).

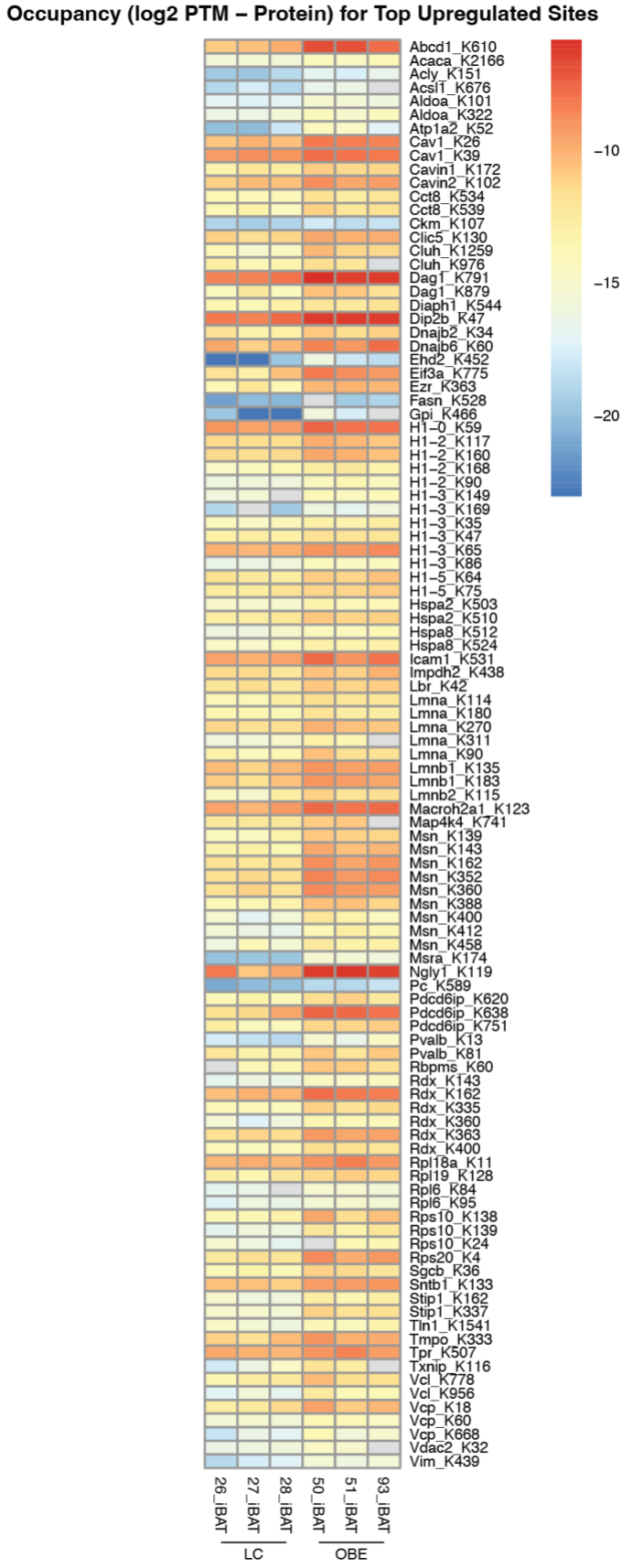

Supplementary Fig. S15 | Occupancy for top 30 GlyGly sites. Ordered (alphabetic) heatmap showing the log2 GlyGly occupancy for the top 30 significantly upregulated sites. LC lean control, OBE obese.

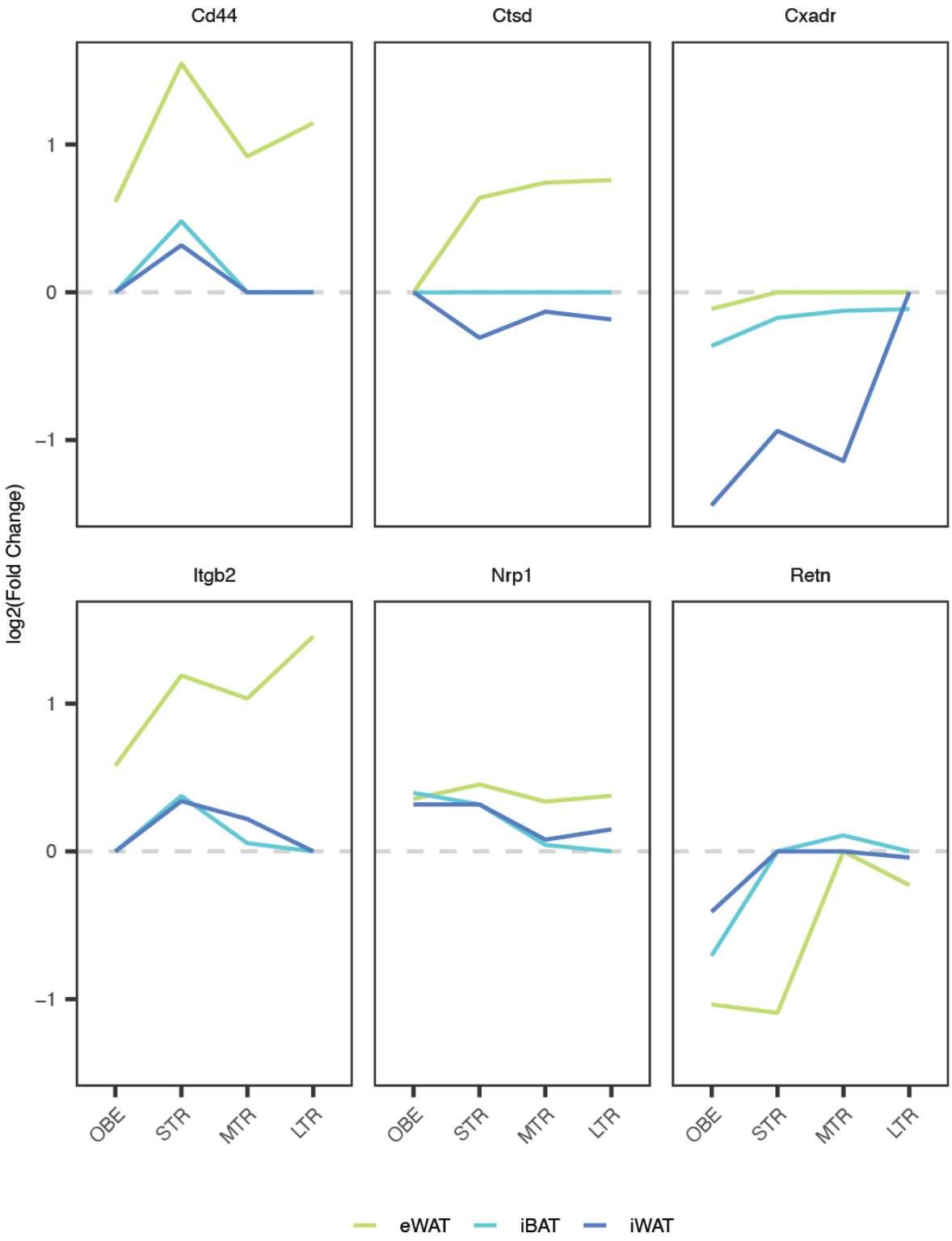

Supplementary Fig. S16 | Adipose tissue-specific differences of potential immune system regulators. Expression profiles showing estimated $\log_2$ fold changes (biological replicates: obesity, n = 5; corresponding lean controls, n = 6; all regression and corresponding control groups, n = 6) for a few selected candidates from our NicheNet analysis results (Fig. 4h,i). OBE obese, STR short-term regression, MTR medium-term regression, LTR long-term regression. Figure was generated using our web application (https://computproteomics.bmb.sdu.dk/app_direct/obesity-atlas/).

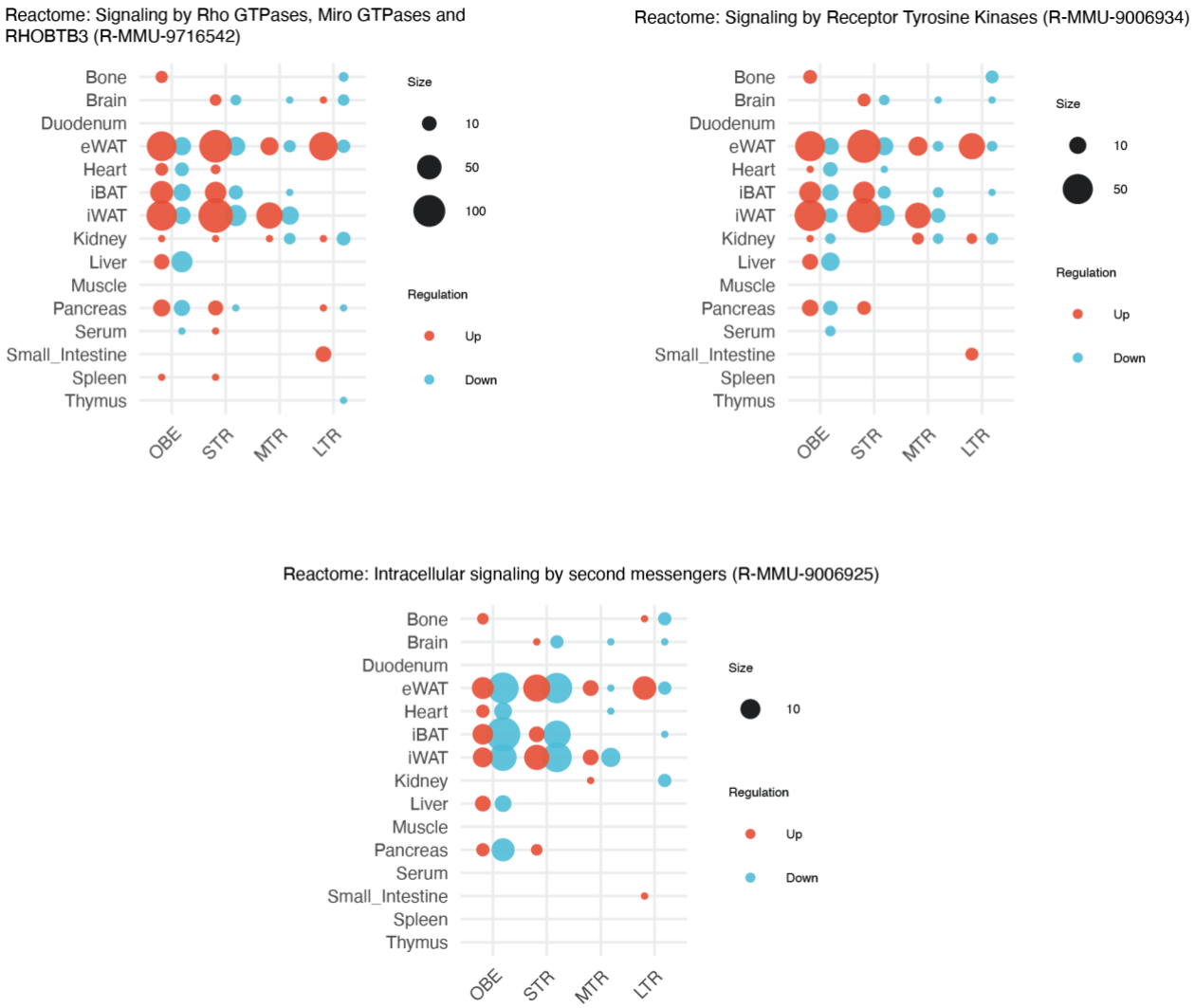

Supplementary Fig. S17 | Exploring system-wide signaling pathways. Dot plots showing the system-wide DEP count for proteins in the Reactome signaling pathways related to 'Rho GTPases' (top left), 'Receptor tyrosine kinases' (top right), and 'Intracellular second messengers' (bottom). OBE obese, STR short-term regression, MTR medium-term regression, LTR long-term regression. Figure was generated using our web application (https://computproteomics.bmb.sdu.dk/app_direct/obesity-atlas/).